

N_8^- Polynitrogen Stabilized on Multi-Wall Carbon Nanotubes for Oxygen-Reduction Reactions at Ambient Conditions**

Zhiyi Wu, El Mostafa Benchafia, Zafar Iqbal,* and Xianqin Wang*

Abstract: Polynitrogen (PN) species (N_n , n from 3 to 8) as highly energetic materials have attracted many theoretical calculations and predictions. N_3 , N_4 , N_5 or their ions were experimentally detected under high-pressure and high-temperature conditions. Herein, a N_8^- PN stabilized on the positively charged sidewalls of multi-walled carbon nanotubes (MWNTs) has been synthesized using cyclic voltammetry (CV) under ambient conditions. ATR-FTIR and Raman spectroscopic data assigned on the basis of density functional theory (DFT) calculations support the successful synthesis of a C_{2h} symmetry chain structure of the N_8 anion stabilized as $MWNT^+N_8^-$. Temperature programmed desorption (TPD) data show that $MWNT^+N_8^-$ is thermally stable up to 400°C. Oxygen-reduction reaction (ORR) experiments carried out using $MWNT^+N_8^-$ as the cathodic catalyst shows that it is very active for ORR with an even higher current density than that of a commercial Pt/carbon catalyst.

Polynitrogen (PN) species (N_n , n from 3 to 8) and compounds are chain-like arrangements of nitrogen atoms that are building blocks for three-dimensional crystalline structures.^[1] Pure polynitrogen solids are particularly attractive because of their high energy density and decomposition to an inert gas that is non-toxic and friendly to the environment. Recent ab initio and molecular dynamics calculations suggested that charge-transfer interactions between carbon nanotube (CNT) sidewalls and polynitrogen compounds could stabilize polynitrogen compounds at ambient conditions.^[2] Density functional theory (DFT) has been used to show that a N_8 single zigzag chain of nitrogen atoms is stable

inside carbon nanotubes and between sheets of graphene.^[3] A novel approach to the isolation of a polynitrogen phase that would be stable at ambient conditions is suggested by the work of Abou-Rachid et al.^[4] (see Figure S1 in the Supporting Information). Owens however predicted with DFT calculations that a double chain $(N_2)_{12}$ oligomer would be stable under ambient conditions without carbon nanotube or graphene sheets.^[5] More recently, Hirshberg et al. used DFT-based theoretical methods to predict a stable molecular crystal of N_8 that is more stable than other N_n polynitrogen species (see Figure S2).^[6]

Since the first synthesis of the azide anion N_3^- in 1890, it has been the only known stable homoatomic nitrogen species for more than 100 years besides molecular N_2 .^[1] Although theoretical studies have predicted the existence of other polynitrogen compounds and intense efforts have been made to synthesize them,^[7] it was not until the last decade that N_5^+ was synthesized for the first time.^[8] This led to extensive research resulting in the synthesis or gas-phase detection of several other species, such as N_5^- , N_3 , and N_4 .^[9–11] One cubic gauche (cg) form was experimentally observed at high pressure (see Figure S3).^[7] The structure formed however dissociated under ambient conditions and could not be recovered.^[12] Another report suggested the existence of a polynitrogen phase in sodium azide, (NaN_3) subjected to a pressure of 160 GPa at temperatures ranging from 120 K to 3300 K.^[12] Macroscopic synthesis of polynitrogen compounds, however, remains difficult owing to their intrinsic instability. Moreover, no molecular solid consisting of pure N_n species has been identified or synthesized experimentally to date.^[1] Herein, a novel N_8^- polynitrogen phase stabilized on the positively charged sidewalls of MWNTs has been synthesized for the first time using cyclic voltammetry (CV) at ambient conditions, and tested for the oxygen-reduction reaction (ORR). To our knowledge, there has been no previous report of polynitrogen-based electrocatalysts.

To synthesize a $MWNT^+N_8^-$, CV was carried out using a three-electrode set up using a computer-controlled potentiostat–galvanostat. As shown in Figure 1, a clear oxidation peak of azide anion at around 0.58 V was observed during CV synthesis. The peak was stable for all the CV cycles. An oxidation peak was not detected without MWNTs suggesting that the azide ions are irreversibly oxidized to azide radicals which can form long and well-ordered polynitrogen species on the positively charged MWNTs. The reaction pathway can be denoted as: $N_3^- \rightarrow N_3^* \rightarrow [N-N-N]_n$. The downward peak in solid curve in Figure 1 already shows the ORR activity of the synthesized polynitrogen. 12 CV cycles were recorded (Figure S4). When the number of cycles increases, the oxidation peak gets weaker owing to the decreasing azide concentration

[*] Z. Wu, E. M. Benchafia

Department of Materials Science and Engineering
New Jersey Institute of Technology
Newark, NJ 07102 (USA)

Prof. Dr. Z. Iqbal

Department of Chemistry and Environmental Science
New Jersey Institute of Technology
Newark, NJ 07102 (USA)
E-mail: zafar.iqbal@njit.edu

Prof. Dr. X. Q. Wang

Department of Chemical, Biological and Pharmaceutical
Engineering, New Jersey Institute of Technology
Newark, NJ 07102 (USA)
E-mail: xianqin.wang@njit.edu

[**] We thank the Max Planck Institute of Colloids and Interfaces (Germany) for providing a carbon nitride reference sample. The work was supported by an NSF CBET 1231682 grant and partially by an ACS-PRF 53582-ND10.

Supporting information for this article is available on the WWW under <http://dx.doi.org/10.1002/anie.201403060>.

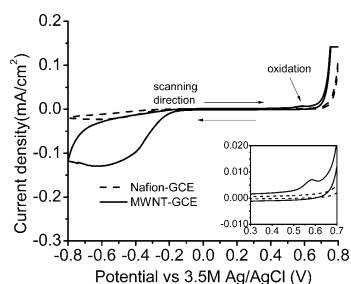


Figure 1. CV during polynitrogen phase synthesis on MWNT-GCE (glassy carbon electrode) working electrode in 2 M sodium azide dissolved in pH 4 buffer solution. Stable curves with potential versus Ag/AgCl were recorded for at least 12 CV cycles (See Figure S4). The GCE working electrode was prepared without MWNT and used as the reference. Inset: expansion of the oxidation region.

in solution and the oxygen reduction peak becomes stronger because there is more polynitrogen synthesized on the MWNTs.

Attenuated total reflectance Fourier transform infrared (ATR-FTIR) spectra in Figure 2 show a clear signal near 2050 cm^{-1} from a polynitrogen-MWNT sheet 2M. This signal was not detected in pristine MWNT, dipped MWNT sheet 2M,

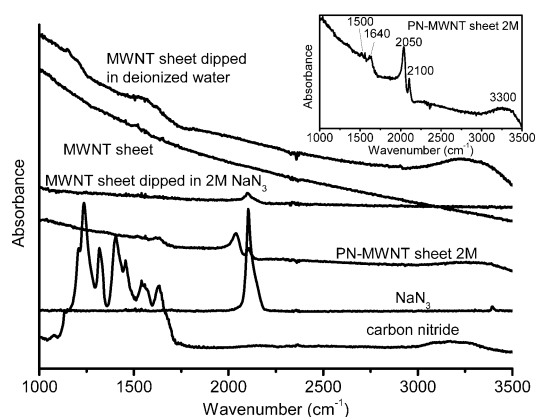


Figure 2. ATR-FTIR spectra in the 1000 to 3500 cm^{-1} range. The MWNT background has been subtracted from the MWNT containing samples. PN-MWNT sheet = polynitrogen-MWNT sheet.

NaN_3 or carbon nitride.^[13] The signals around 1500 cm^{-1} and 1640 cm^{-1} together with the broad feature at 3300 cm^{-1} are from residual water trapped in the MWNT sheet, which is consistent with the IR spectra for the MWNT sheet dipped in deionized water and dried in air. The band near 2100 cm^{-1} can be assigned to the azide ion asymmetric stretching mode from residual sodium azide. The characteristic modes of carbon-nitrogen bonding below 1800 cm^{-1} from carbon nitride^[14] were not detected from the polynitrogen-MWNT sheet 2M, which indicates a difference in structure between polynitrogen on MWNT and a nitrogen-doped carbon structure. The Raman spectra in Figure 3 clearly depict a line at 1080 cm^{-1} from polynitrogen-MWNT sheet 2M which was not detected from the MWNT sheet or from the dipped MWNT sheet 2M. The weak, sharp feature at 2150 cm^{-1} is likely to be extrinsic.

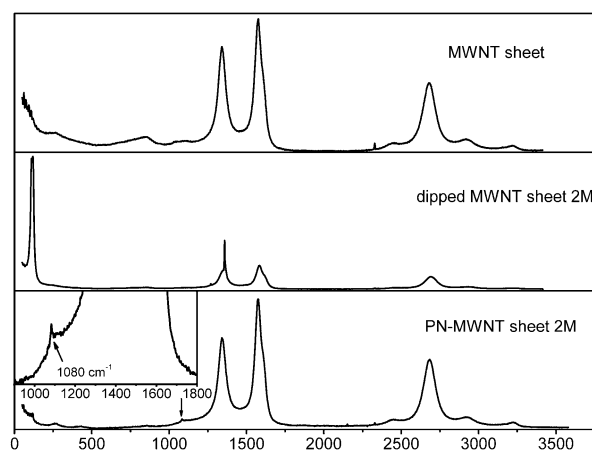


Figure 3. Raman spectra in the 1000 to 2300 cm^{-1} spectral range using 10 mW 514.5 nm laser excitation.

ATR-FTIR and Raman spectra for the polynitrogen-MWNT sheet 2M indicate that the vibrational modes of the synthesized material are very close to the DFT calculation results (Table S1) for the $\text{N}_8^- \text{C}_{2h}$ structure (Figure 4).

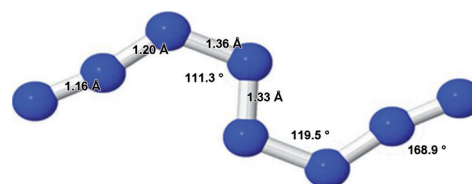


Figure 4. DFT minimized C_{2h} symmetry linear-chain structure of the N_8 anion.

Our DFT calculations were carried out at the 6-31 + G (d, p) level using GamessUS.^[15,16] We chose to adopt the B3LYP functional with the 6-31 + G (d, p) as it gave us the best results for the established N_3^- azide ion. IR intensities are in $\text{debye}^2\text{amu}^{-1}\text{Å}^{-2}$ while Raman intensities are expressed in $\text{Å}^4\text{amu}^{-1}$. The azide anion N_3^- structure optimization carried out in this study was for the sole purpose of validation of our method. There is a deviation of 2.9% for the main IR N_3^- anti-symmetric stretching frequency at 2160 cm^{-1} which is observed experimentally at 2100 cm^{-1} , while we recorded a deviation of only 0.29% for the N_3^- symmetric stretching Raman frequency at 1364 cm^{-1} , which is observed experimentally at 1360 cm^{-1} . Based on the calculation, the N_8^- vibrational frequencies with the highest IR and Raman intensity are predicted at 2057 cm^{-1} and 1060 cm^{-1} (Table S1), respectively, which are in good agreement with the experimental values of 2050 cm^{-1} and 1080 cm^{-1} in Figures 2 and 3, respectively, and an earlier calculation by Bartlett et al.^[17–20] The IR and Raman results coupled with DFT calculations show that a polynitrogen oligomer anion stabilized by MWNT cationic counterions has been synthesized successfully.

As-prepared carbon nanotube sidewalls are hole-doped or positively charged as a result of reaction with oxygen in air to

form oxygen anions or by intercalation of the Na^+ between the graphitic layers of MWNT sidewalls. The structure of the N_8 anion can be derived from the structure of a neutral N_8 cluster from the N_8 molecular crystal proposed by Hirshberg et al.^[6] depicted in Figure S3. We also calculated the vibrational modes of the N_8 neutral cluster with the same method. The results from our calculation agree with the results of Hirshberg et al.^[6] (Table S1–S3, Figure S5–S7). Compared to the neutral N_8 cluster, the IR active stretching $\text{N}=\text{N}$ vibrational mode from N_8^- is shifted to lower frequencies because of an increase in the calculated bond length of the anion cluster (Figure 4) relative to that of the neutral cluster. This is consistent with the computed increase in charge density around the end nitrogen-nitrogen bonds of the neutral N_8 cluster molecule (Figure S5).^[6]

To confirm the thermal stability of the sample, temperature programmed desorption (TPD) was carried out. The result is compared to those from the dipped-MWNT sheet 2 M and carbon nitride samples in Figure 5. The TPD scan of the

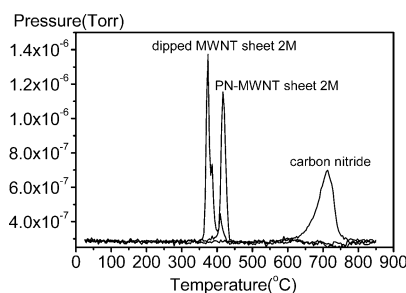


Figure 5. N_2 signals from TPD scans. The curves have been normalized by sample weight.

polynitrogen-MWNT sheet 2 M show that the polynitrogen species on the carbon nanotube substrate is thermally stable and it decomposes to nitrogen at a temperature above 400 °C. Three N_2 peaks are detected for the dipped-MWNT sheets, which may correspond to azide deposited on the outer-, intra-, and inter-layers of the nanotubes in the MWNT sheet. Carbon nitride decomposes at a much higher temperature, above 600 °C by the breaking of C–N bonds. It is thus clear that more ordered polynitrogen species are formed on the MWNTs during the CV process. No carbon nitride species are detected on the polynitrogen-MWNT sheet.

The electrocatalytic activities for ORR with the samples were measured using linear-sweep voltammetry (LSV) with O_2 saturated or N_2 purged 0.1 M KOH as the electrolyte. A clear cathodic current was detected under O_2 , which corresponds to oxygen reduction, while there is a much less obvious response near the potential with the N_2 purged electrolyte (Figure 6, top). The response under N_2 could be attributed to the reduction of residual O_2 in the electrolyte or oxygen occluded in the pores of MWNT.^[21,22] Recently, multi-walled carbon nanotubes have been reported to have some intrinsic ORR activity^[23] as also shown by our ORR results (Figure 6, bottom). Comparing with dipped MWNT sheet 2 M, which shows some ORR activity with the onset potential at around –0.2 V, the polynitrogen-MWNT sheet 2 M shows a more

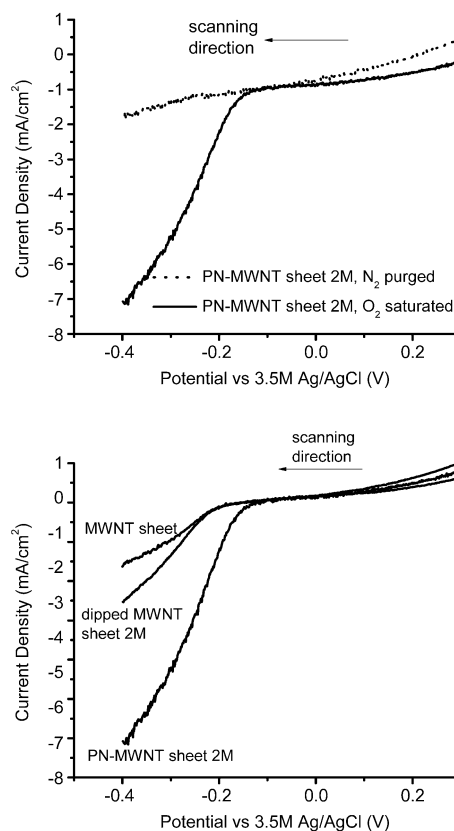


Figure 6. ORR results in 0.1 M KOH with linear-sweep voltammetry. Top: ORR with N_2 purged and O_2 saturated electrolyte. Bottom: ORR with MWNT sheet, dipped MWNT sheet 2 M, and PN-MWNT sheet 2 M, using O_2 saturated electrolyte.

positive onset potential (–0.14 V) and higher current density. The improved ORR performance could be attributed to the electron lone pairs of N in the N_8^- polynitrogen species. The determination of the active sites for ORR and the roles that nitrogen plays in nitrogen-carbon based catalysts has been controversial for a long time. DFT calculations have suggested that the catalytic ORR activity is either because of charge-transfer interactions between nitrogen and adjacent carbon atoms, leading to oxygen chemisorbed on the carbon atoms and weakening of O–O bonding for further reduction of oxygen,^[24] or oxygen bonding with the lone pair electrons of doped nitrogen atoms on carbon substrate.^[25] Our ORR results indicate that a N–N unit from N_3^- or in the N_8^- polynitrogen species can play the role as the active site for ORR, which has not been reported previously. Natural bonding orbital (NBO) analysis is used to calculate the partial charge distribution on N_8^- species. Based on the charge distribution, the most active sites should be N1 and N2 that have more negative charges (Figure S8).^[26]

We also investigated polynitrogen synthesized with different azide concentrations. As shown in Figure 7 (Table S4), with the increasing of azide concentration, both the nitrogen desorption temperatures for dipped MWNT sheet and polynitrogen-MWNT sheet shift to lower temperatures, which indicates an increasing amount of weaker attached nitrogen compounds as the azide concentration increases. Indeed,

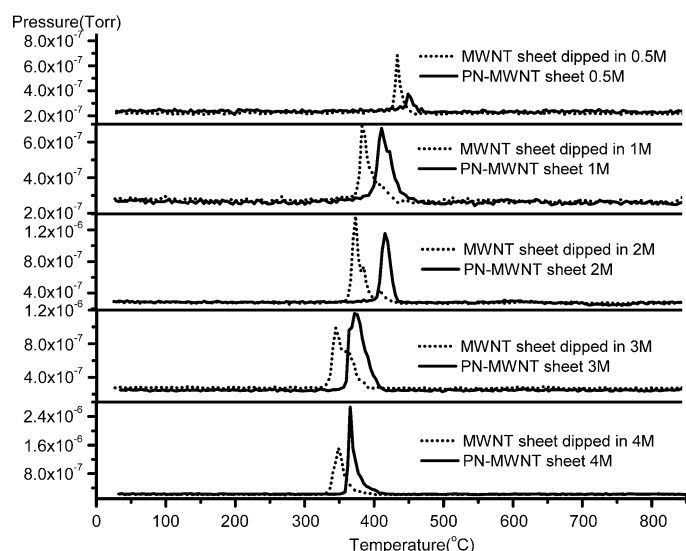


Figure 7. N^{14} signals normalized by sample weight from the TPD results for dipped MWNT and polynitrogen-MWNT sheets with different azide concentrations for electrochemical synthesis.

nitrogen compounds tend to occupy the sites that will form stronger interactions with MWNT to give a lower overall free energy. For the dipped MWNT sheets, initially the nitrogen-desorption amount increases with the increasing azide concentration, but the desorption amount does not change much from 2M to 4M, which suggests the saturation of the sites within the MWNT. However, nitrogen desorption amount for polynitrogen-MWNT continuously increases with the increasing of azide concentration, suggesting more polynitrogen is formed with higher azide concentrations from 0.5M to 4M. This is further supported by FTIR results in Figure 8, which shows that the relative intensity of the peak at around 2050 cm^{-1} continuously increases with the increase in the azide concentration. The concomitant decrease in the intensity of the band at 2100 cm^{-1} for the azide ion with increasing azide ion concentration is because increased N_8^- formation results in the MWNT surfaces becoming increasingly inaccessible for azide ion adsorption. To compare the ORR performance of the samples synthesized with different azide concentrations and also to compare with commercial Pt/C

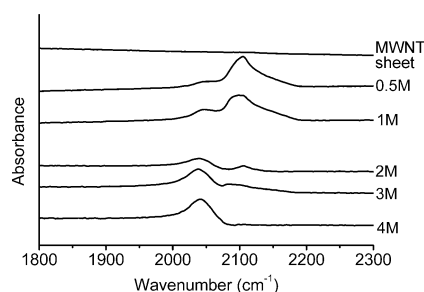


Figure 8. FTIR spectra in the $1800\text{--}2300\text{ cm}^{-1}$ region for polynitrogen-MWNT sheets after electrochemical synthesis with different azide concentrations. MWNT background has been subtracted for the polynitrogen-MWNT curves.

catalyst, polynitrogen-MWNT-GCE and Pt/C-GCE were prepared and the results are shown in Figure 9. The result from Pt/C is consistent with Gong's work.^[24] The current densities with the polynitrogen-MWNT samples increase with the increasing of azide concentration, suggesting a facilitating of oxygen reduction with larger amounts of N_8^- polynitrogen. Compared to Pt/C, polynitrogen-MWNT has a more negative

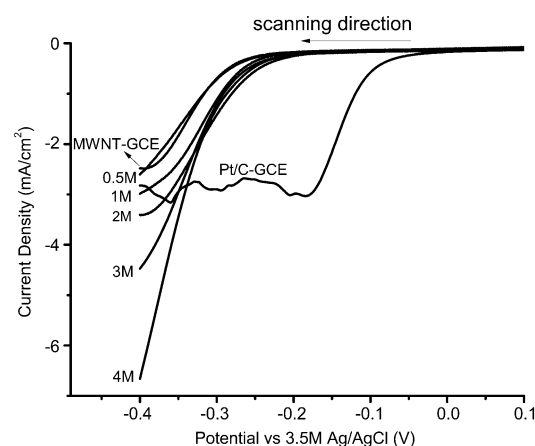


Figure 9. ORR results in 0.1 M KOH for polynitrogen-MWNT-GCE, synthesized with different azide concentrations, and for a commercial Pt/C catalyst. Pt/C-GCE was prepared by the same method as for MWNT-GCE, except that 10% platinum on Vulcan XC-72 (E-Tek) was deposited. LSV scan rate: 100 mV s^{-1} .

onset potential, but higher current density for polynitrogen-MWNTs synthesized with an azide concentration higher than 1M. The results suggest that a higher power output can be achieved over $\text{MWNT}^+\text{N}_8^-$ than on a Pt/C commercial cathodic catalyst. The current density with the polynitrogen sample during the 4 scans (Figure S9) shows that polynitrogen is relatively stable during ORR. It therefore has the potential to replace Pt as a catalyst in fuel cells.

In summary, we have successfully synthesized a polynitrogen anion stabilized on the sidewalls of MWNTs by a CV method for the first time. The polynitrogen-MWNT functions as a metal-free ORR catalyst. A $\text{N}_8^- \text{C}_{2h}$ structure is confirmed by ATR-FTIR, Raman spectroscopy and DFT calculation results, and consistent with recent DFT findings from Bartlett et al.^[17–20] and Hirshberg, et al.^[6] TPD results show that the N_8^- polynitrogen structure is thermally stable to about 400°C . ORR experiments suggest that N–N sites from the polynitrogen materials or azide ions are active in a KOH electrolyte. With increasing azide concentrations from 0.5M to 4M for the electrochemical synthesis, a larger amount of polynitrogen is obtained on the MWNTs, leading to increased ORR activity. Although it has a more negative onset potential, the current density of $\text{MWNT}^+\text{N}_8^-$ is higher than that of a commercial Pt/C electrode. This work therefore opens the door to the synthesis of other polynitrogen materials, and their potential use as high energy and ORR catalytic materials.

Experimental Section

To synthesize polynitrogen materials on MWNTs CV was carried out using a computer-controlled CH Instruments 832C potentiostat-galvanostat on -COOH functionalized multi-walled carbon nanotubes (MWNTs, purchased from Nanolab). CV was performed with a three-electrode setup. The working electrode was dipped in 40 mL 0.5–4 M NaN_3 (Aldrich) dissolved in a buffer solution (pH 4.0), which was used as the electrolyte. Pt and Ag/AgCl were used as the counter electrode and standard reference electrode, respectively. CV was also carried out on MWNT-GCE without NaN_3 in the solution to clarify the oxidation peak from N_3^- (Figure S10). TPD was carried out using a Micromeritics AutoChem II 2920 system. FTIR was carried out using a Nicolet ThermoElectron FTIR spectrometer combined with a MIRacle ATR platform assembly and a ZnSe plate, and denoted as ATR-FTIR. Raman spectroscopy was performed with a Thermo Scientific DXR Raman microscope. For ORR, PN-MWNT sheets and the dipped-MWNT sheets were cut into strips, each of which had approximately the same surface area and used as the working electrode. Pt and Ag/AgCl were used as the counter electrode and reference electrode, respectively. 0.1 M KOH solution was used as the electrolyte. DFT calculations were carried out by density functional theory at the 6-31 + G (d, p) level using GamessUS. We chose to adopt the B3LYP functional with the 6-31 + G (d, p) as it gave us the closest results for the established azide ion. (See Supporting Information for detailed experimental information).

Received: March 6, 2014

Revised: June 10, 2014

Published online: August 14, 2014

Keywords: electrocatalysis · MWNTs · oxygen reduction reaction · polynitrogen

- [1] M. T. Nguyen, *Coord. Chem. Rev.* **2003**, *244*, 93–113.
- [2] H. Abou-Rachid, A. Hu, D. Arato, X. Sun, S. Desilets, *Int. J. Energ. Mater. Chem. Propuls.* **2008**, *7*, 359–371.
- [3] A. Hu, F. Zhang, T. Woo, *Phys. Rev. B* **2010**, *82*, 125410.
- [4] H. Abou-Rachid, A. Hu, V. Timoshevskii, Y. Song, L.-S. Lussier, *Phys. Rev. Lett.* **2008**, *100*, 196401.
- [5] F. J. Owens, *Comput. Theor. Chem.* **2011**, *966*, 137–139.
- [6] B. Hirshberg, R. B. Gerber, A. I. Krylov, *Nat. Chem.* **2014**, *6*, 52–56.
- [7] P. C. Samartzis, A. M. Wodtke, *Int. Rev. Phys. Chem.* **2006**, *25*, 527–552.
- [8] K. O. Christe, W. W. Wilson, J. A. Sheehy, J. A. Boatz, *Angew. Chem. Int. Ed.* **1999**, *38*, 2004–2009; *Angew. Chem.* **1999**, *111*, 2112–2118.
- [9] A. Vij, J. G. Pavlovich, W. W. Wilson, V. Vij, K. O. Christe, *Angew. Chem. Int. Ed.* **2002**, *41*, 3051–3054; *Angew. Chem.* **2002**, *114*, 3177–3180.
- [10] J. Zhang, P. Zhang, Y. Chen, K. Yuan, S. A. Harich, X. Wang, Z. Wang, X. Yang, K. Morokuma, A. M. Wodtke, *Phys. Chem. Chem. Phys.* **2006**, *8*, 1690–1696.
- [11] F. Cacace, G. de Petris, A. Troiani, *Science* **2002**, *295*, 480–481.
- [12] M. I. Eremets, A. G. Gavriluk, I. A. Trojan, D. A. Dzivenko, R. Boehler, *Nat. Mater.* **2004**, *3*, 558–563.
- [13] X. Wang, K. Maeda, A. Thomas, K. Takanabe, G. Xin, J. M. Carlsson, K. Domen, M. Antonietti, *Nat. Mater.* **2009**, *8*, 76–80.
- [14] J. Zhang, X. Chen, K. Takanabe, K. Maeda, K. Domen, J. D. Epping, X. Fu, M. Antonietti, X. Wang, *Angew. Chem. Int. Ed.* **2010**, *49*, 441–444; *Angew. Chem.* **2010**, *122*, 451–454.
- [15] M. Gordon, M. Schmidt in *Theory Appl. Comput. Chem. First Forty Years* (Eds.: C. Dykstra, G. Frenking, K. Kim, G. Scuseria), Elsevier, Amsterdam, **2005**, pp. 1167–1189.
- [16] M. W. Schmidt, K. K. Baldridge, J. A. Boatz, S. T. Elbert, M. S. Gordon, J. H. Jensen, S. Koseki, N. Matsunaga, K. A. Nguyen, S. Su, et al., *J. Comput. Chem.* **1993**, *14*, 1347–1363.
- [17] W. J. Lauderdale, J. F. Stanton, R. J. Bartlett, *J. Phys. Chem.* **1992**, *96*, 1173–1178.
- [18] R. J. Bartlett, *Chem. Ind.* **2000**, *4*, 140–143.
- [19] S. Fau, R. J. Bartlett, *J. Phys. Chem. A* **2001**, *105*, 4096–4106.
- [20] S. Fau, K. J. Wilson, R. J. Bartlett, *J. Phys. Chem. A* **2002**, *106*, 4639–4644.
- [21] J. N. Barisci, G. G. Wallace, R. H. Baughman, *J. Electrochem. Soc.* **2000**, *147*, 4580–4583.
- [22] G. Che, B. B. Lakshmi, E. R. Fisher, C. R. Martin, *Nature* **1998**, *393*, 346–349.
- [23] Y. Li, W. Zhou, H. Wang, L. Xie, Y. Liang, F. Wei, J.-C. Idrobo, S. J. Pennycook, H. Dai, *Nat. Nanotechnol.* **2012**, *7*, 394–400.
- [24] K. Gong, F. Du, Z. Xia, M. Durstock, L. Dai, *Science* **2009**, *323*, 760–764.
- [25] D. Deng, X. Pan, L. Yu, Y. Cui, Y. Jiang, J. Qi, W.-X. Li, Q. Fu, X. Ma, Q. Xue, et al., *Chem. Mater.* **2011**, *23*, 1188–1193.
- [26] E. D. Glendening, J. K. Badenhoop, A. E. Reed, J. E. Carpenter, J. A. Bohmann, C. M. Morales, C. R. Landis, F. Weinhold, NBO 6.0. (Theoretical Chemistry Institute, University of Wisconsin, Madison, WI, **2013**).